


Article

The Effect of Vanadium Inhalation on the Tumor Progression of Urethane-Induced Lung Adenomas in a Mice Model

Nelly López-Valdez, Marcela Rojas-Lemus  and Teresa I. Fortoul *

Departamento de Biología Celular y Tisular, Facultad de Medicina, Universidad Nacional Autónoma de México (UNAM), México City 04510, Mexico; nellylopezvaldez@gmail.com (N.L.-V.); marcelarojaslemus@hotmail.com (M.R.-L.)

* Correspondence: fortoul@unam.mx; Tel.: +52-55-5623-2182

Abstract: Lung cancer has the highest death rates. Aerosol drug delivery has been used for other lung diseases. The use of inhaled vanadium (V) as an option for lung cancer treatment is explored. Four groups of mice were studied: (1) Saline inhalation alone, (2) Single intraperitoneal (i.p.) dose of urethane, (3) V nebulization twice a week (Wk) for 8 Wk, and (4) A single dose of urethane and V nebulization for 8 Wk. Mice were sacrificed at the end of the experiment. Number and size of tumors, PCNA (proliferating cell nuclear antigen) and TUNEL (terminal deoxynucleotidyl transferase dUTP nick-end labeling) immunohistochemistry were evaluated and compared within groups. Results: The size and number of tumors decreased in mice exposed to V-urethane and the TUNEL increased in this group; differences in the PCNA were not observed. Conclusions: Aerosol V delivery increased apoptosis and possibly the growth arrest of the tumors with no respiratory clinical changes in the mice.

Keywords: urethane; vanadium; aerosol delivery; lung cancer; apoptosis; antineoplastic



Citation: López-Valdez, N.; Rojas-Lemus, M.; Fortoul, T.I. The Effect of Vanadium Inhalation on the Tumor Progression of Urethane-Induced Lung Adenomas in a Mice Model. *Inorganics* **2021**, *9*, 78. <https://doi.org/10.3390/inorganics9110078>

Academic Editor: Dinorah Gambino

Received: 9 October 2021

Accepted: 27 October 2021

Published: 29 October 2021

Publisher's Note: MDPI stays neutral with regard to jurisdictional claims in published maps and institutional affiliations.



Copyright: © 2021 by the authors. Licensee MDPI, Basel, Switzerland. This article is an open access article distributed under the terms and conditions of the Creative Commons Attribution (CC BY) license (<https://creativecommons.org/licenses/by/4.0/>).

1. Introduction

Lung cancer is a worldwide health problem, and this tumor has the highest estimated death rates because of the delay in the diagnosis and in the beginning of its treatment [1]. Usually, the patients have been mistreated because they do not have a previous history of smoking, which is the reason why lung cancer is not the first suspected diagnosis, even though its frequency among this group of patients has steadily increased. Some of the risk factors reported among non-smokers are environmental and occupational exposures, sex hormones, and wood smoke exposure [2,3]. The main histological subtype observed in recent years is adenocarcinoma [4].

Lung cancer treatment depends on the size of the tumor, the histologic type, and the clinical variables. Surgery, radiotherapy, and chemotherapy and or its combinations are the treatment options. The 5-year relative survival rate is about 17% for all patients and all of the stages of this pathology; if the disease is detected in early stages, the survival rate increases to 54%. Nonetheless, only 15% of the cases are diagnosed at early stages [5]. In addition, the resistance to chemotherapy and the cost of the new options, oriented to specific molecular targets, is expensive [4,6,7]. On the other hand, resistance to these treatments has also increased [8]. Additionally, because of these described events, it is important to keep looking for new treatment options for lung cancer.

The urethane model for lung tumors is a chemical carcinogenesis method that has been used to study tumor progression and treatments [9–11].

Metal compounds have been tested as possible antineoplastic agents, such as platinum compounds. Vanadium (V) is a transitional element with controversial effects [12]. Vanadium compounds have emerged as possible options for therapeutic uses because of the induction of reactive oxygen species (ROS), the activation of apoptotic cell death mechanisms, autophagy, and the inhibition of cell proliferation [13–15]. As antineoplastic

agents, organic compounds have been studied *in vitro* in a variety of cancer types such as pancreatic ductal carcinoma [16].

Recently other optional routes for drug delivery have been proposed for the treatment of diverse pathologies [17] such as lung cancer [11]. Hamzawy et al. reported intratracheal administration of temozolomide in lung tumors induced by urethane [18] and Roger-Parra intranasally delivered anti-collagen-V for lung cancer treatment with promising results [11].

Aerosol drug delivery has been a technique used for the treatment of a variety of diseases and recently for experimental antineoplastic therapies [11]. This route increases the bioavailability and decreases the time of action because the doses decrease the risk of side effects, and the drug reaches the lung tissue without the metabolic changes that occur in the liver [19,20]. These benefits have been observed in asthma, COPD, and some lung infections [21,22]. In this study, we explore the administration of V by inhalation as a possible alternative route for the treatment of lung cancer in the urethane-induced lung tumor mice model.

2. Results

During the whole experiment, no signs or changes in the patterns of food intake and water consumption were observed. Body weight was statistically different when comparing the beginning (T0) with the end of the experiment (8th week) in each group. Body weight at 8th week was not statistically different among group I (control), group II (urethane), and group IV (urethane-V). In group III (vanadium), weight was significantly higher compared with the control, urethane, and urethane-V mice groups (Figure 1).

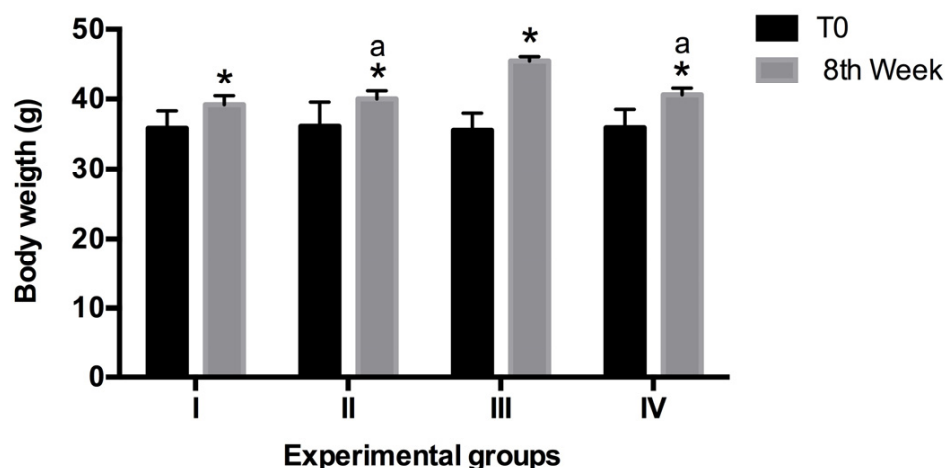


Figure 1. Weight of the mice per group. The weight at the beginning (Time 0) compared to the end of the experiment (8th week) was different. In group III (vanadium) the weight gain was higher than in the other groups. N = 10, values are expressed as the mean of body weight \pm SEM in grams (ANOVA $p \leq 0.05$ Tukey's post hoc). * statistically significant differences vs. T0; a: statistically significant differences versus group III 8th week.

Except in group III (vanadium) where an increase in the weight of the mice was recorded, no other changes in the physical appearance or motor behavior of the animals were observed.

2.1. Lung Histology

Panoramic photomicrographs show the presence of pulmonary adenomas in mice treated with urethane, i.e., groups II and IV (Figure 2B,D, respectively). Groups I and III did not develop lung adenomas (Figure 2A,C, respectively).

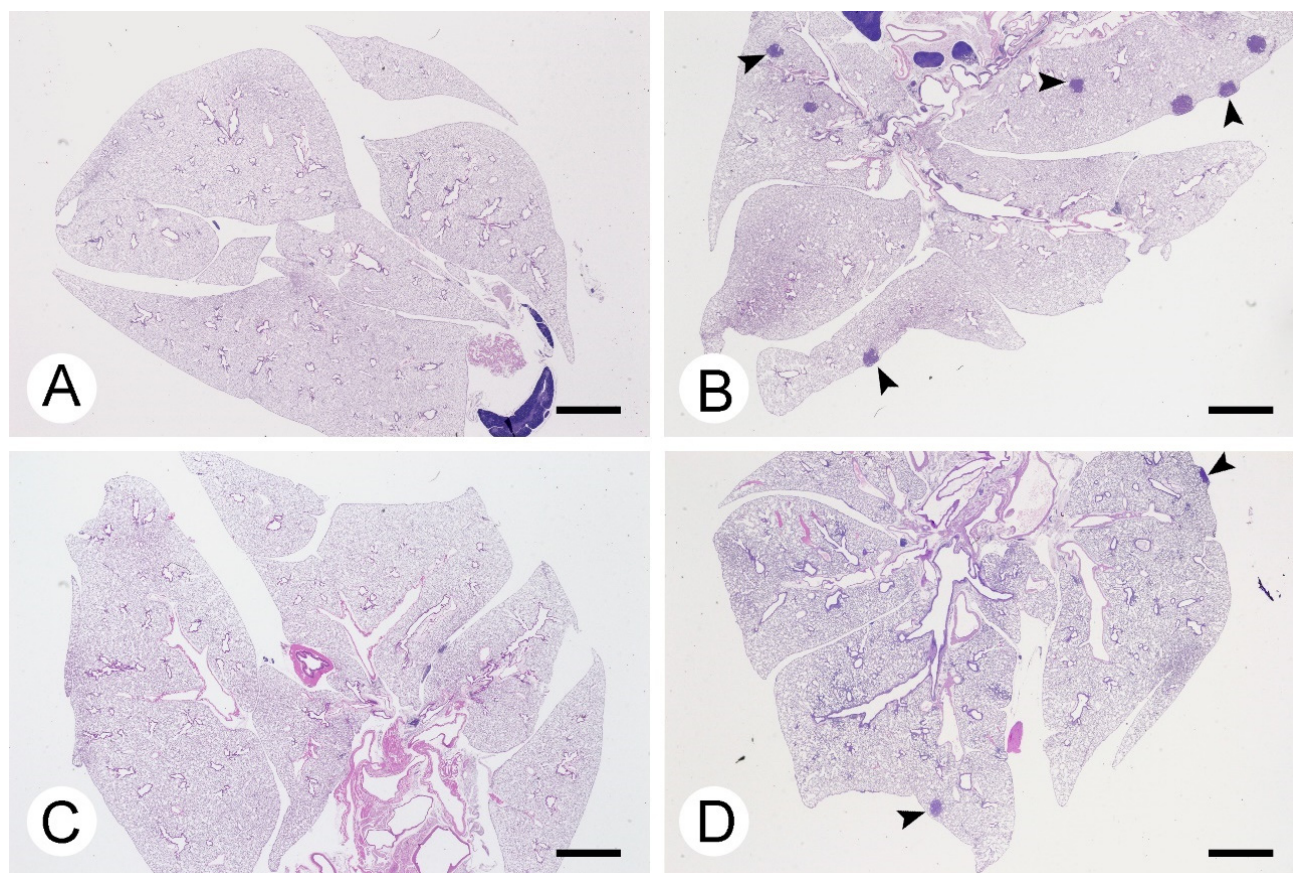


Figure 2. Adenoma development in mice treated with urethane. No tumors are observed in the control (A) and in vanadium (C) groups. Arrow heads (►) indicate the adenomas in urethane (B) and urethane–vanadium (D) groups. Hematoxylin–Eosin. Bar 2 mm.

Detailed changes in the lung tissue observed in the experimental groups are shown in Figure 3. In group I (Figure 3A), bronchioles and alveolar walls with a well-preserved structure were observed; inflammatory foci as well as focal hyperplasia of the bronchiolar and alveolar epithelium, as well as solid adenomas, are clearly identified in group II (Figure 3B). In the V-exposed group (group III; Figure 3C), perivascular and peribronchiolar lymphocytic inflammatory infiltrate were observed, whereas no adenomas were identified; in the urethane–V group (group IV), focal bronchiolar epithelial hyperplasia, small and scanty adenomas, and lymphocytic infiltrate were the main observed features (Figure 3D).

The mean number of tumors in group II was 9 ± 1.13 , whereas in group IV it was 2 ± 0.51 ; when both groups were compared, a statistically significant difference was observed (Figure 4).

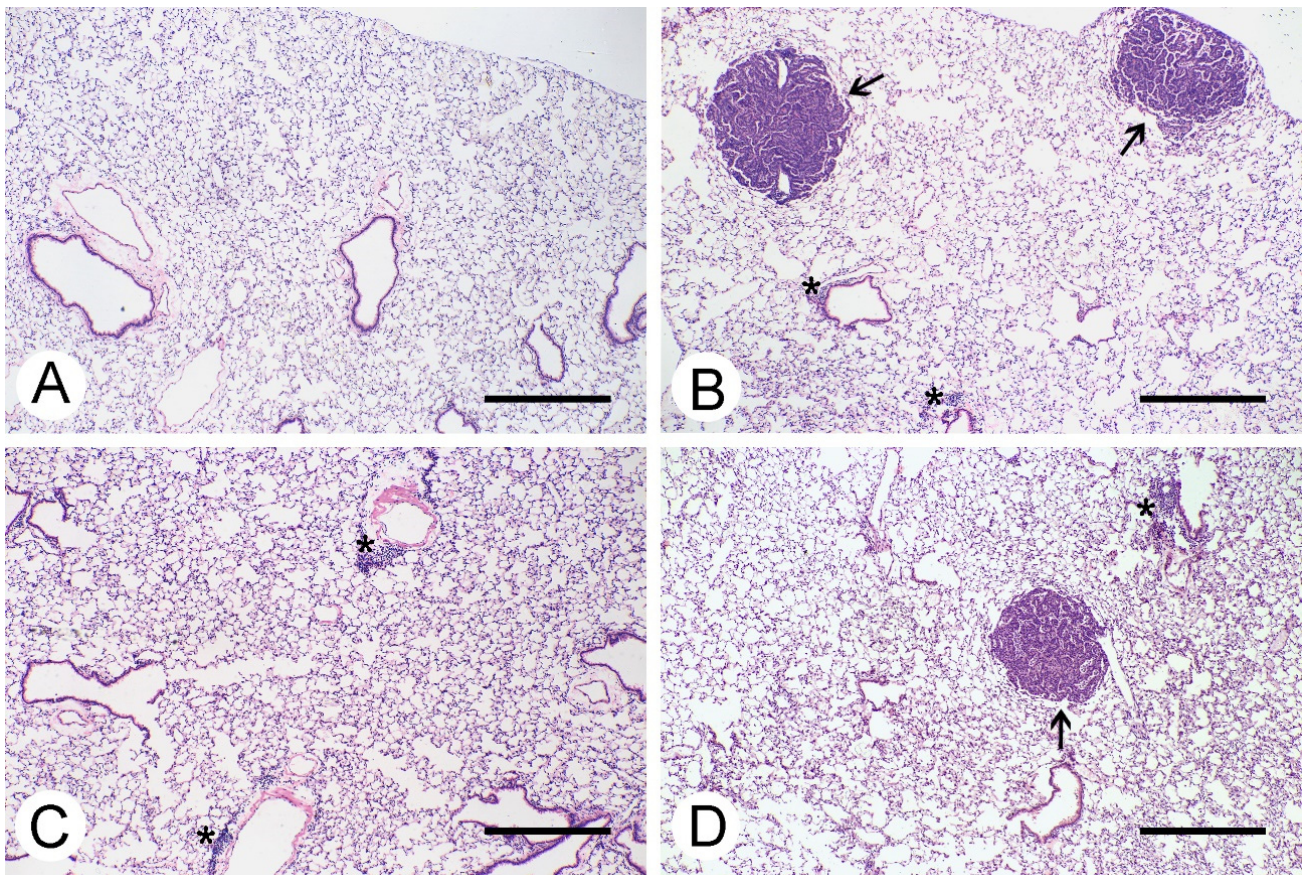


Figure 3. Details of the changes observed in the lungs. Control group (A) with no changes in the lung's parenchyma, whereas in the V-exposed group (C) epithelial hyperplasia and inflammatory infiltrate (*) are observed. In urethane (B) and urethane-V (D) groups, the adenomas (↑) are observed as well as the hyperplastic epithelium (*). Hematoxylin–Eosin stain. Bar 0.5 mm.

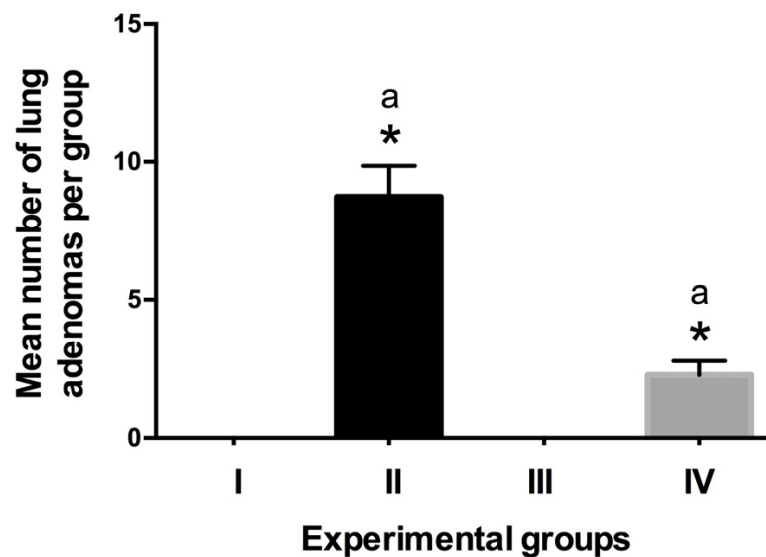


Figure 4. Quantitation of developed adenomas per group. No tumors were observed in group I (control) and group III (vanadium). In group II (urethane), the tumors were larger than in group IV (urethane-V group). N = 10, values are expressed as the mean number of adenomas \pm SEM (ANOVA $p \leq 0.05$ Tukey's post hoc). * Statistically significant differences versus group I; a: statistically significant differences between group II and IV.

The area occupied by tumors in group II was $0.6 \pm 0.07 \text{ mm}^2$, whereas in group IV it was $0.39 \pm 0.05 \text{ mm}^2$, a difference which was statistically significant (Figure 5). No qualitative differences were observed in the amount and the spread of the infiltrate in groups II and IV.

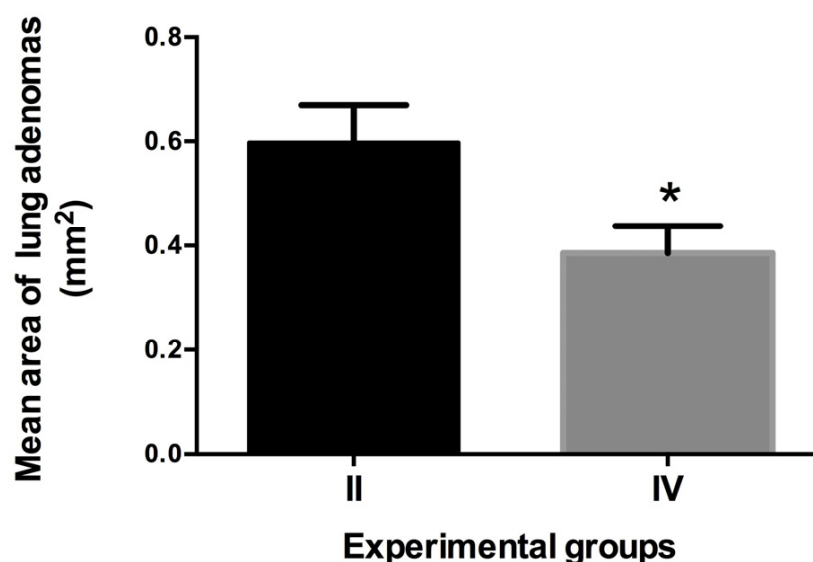


Figure 5. Area (mm^2) occupied by lung adenomas. In group II (urethane) the adenomas were larger compared with those observed in group IV (urethane-V). $N = 10$, values expressed as the mean area \pm SEM (two-tailed Student's *t*-test with Welch's correction, $p \leq 0.05$). * Statistically significant differences between group II versus group IV.

2.2. Proliferative Index

PCNA positive nuclei stain in the lung parenchyma was observed in the four groups. In group I, the positive cells were observed mainly in some bronchiolar cells as well as in group IV. In groups II and IV, the nuclei stain was in the tumor cells (Figure 6) and no statistical difference was observed in the proliferative index calculated only in the adenomas in groups II (PI 24.18%) and IV (PI 25.93%) (Figure 7).

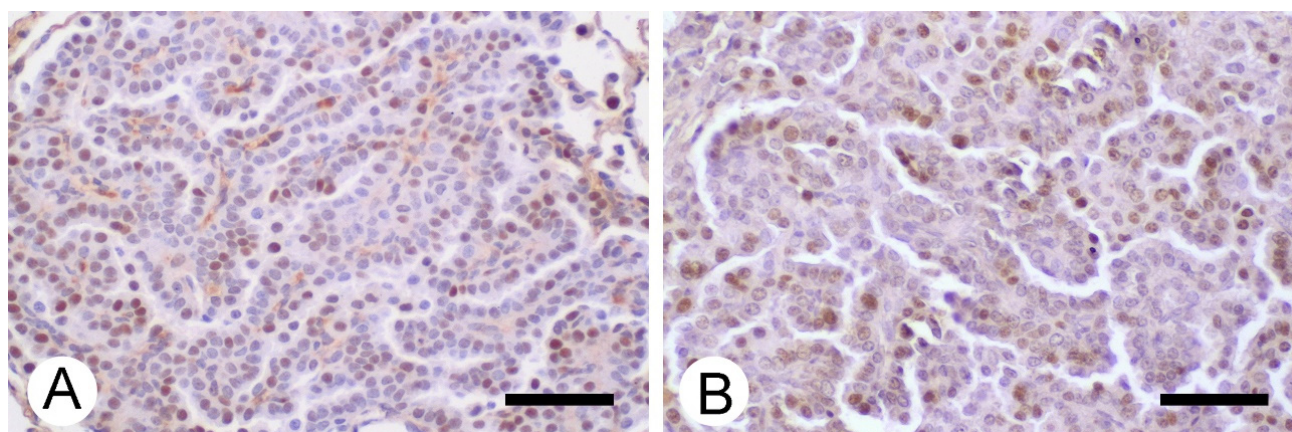


Figure 6. Immune stain for PCNA in lung adenomas. Positive PCNA nuclei (ochre color) were observed in urethane (A) and urethane-V (B) with no statistical difference between them. Hematoxylin counterstain. Bar 50 μm .

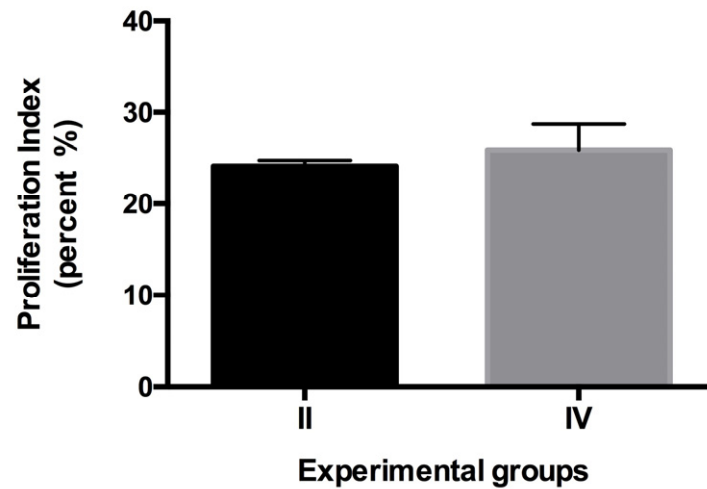


Figure 7. Proliferation index. The index indicated that between groups II and IV, no statistical difference was observed. N = 10, values expressed as mean percentage of PCNA positive nuclei \pm SEM (two-tailed Student's *t*-test with Welch's correction). No statistically significant differences were observed.

2.3. TUNEL Assay

Positive TUNEL nuclei stain in the lung parenchyma was observed in the four groups. In group I, the positive cells were scanty inflammatory cells in the parenchyma, whereas in the V-exposed group (III), the stain was in the inflammatory cells and scarce in the bronchiolar epithelia. In groups II and IV, the nuclei stain was in the tumor cells, the inflammatory foci, and in the bronchiolar epithelium (Figure 8).

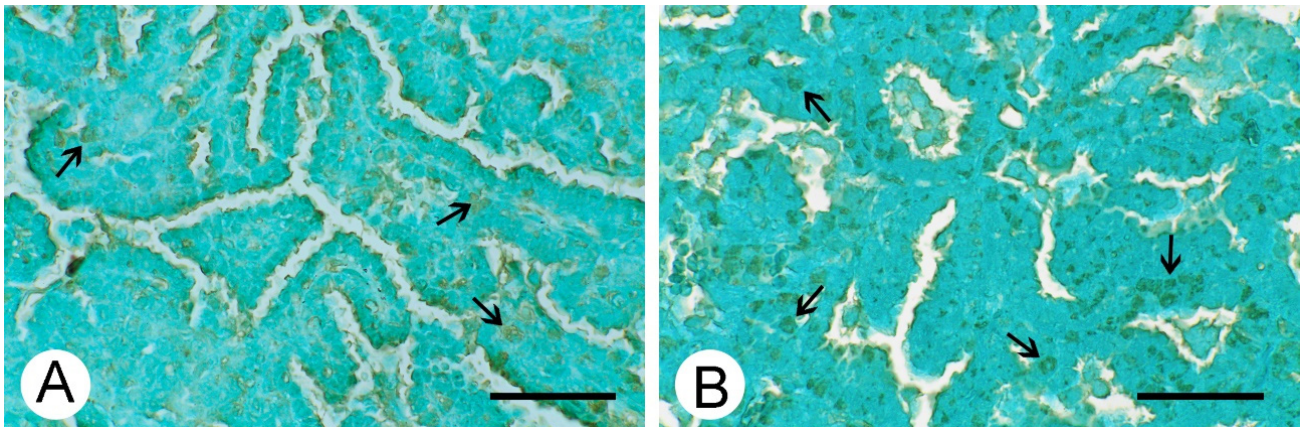


Figure 8. TUNEL immuno-assay. Positive nuclei TUNEL stain (ochre color) were observed in urethane group (A) and urethane-V group (B) (\uparrow). Light green counterstain. Bar 50 μ m

A clear statistical difference was observed in the apoptotic index calculated only in the adenomas in groups II (AI 5.1%) and IV (AI 10%) (Figure 9).

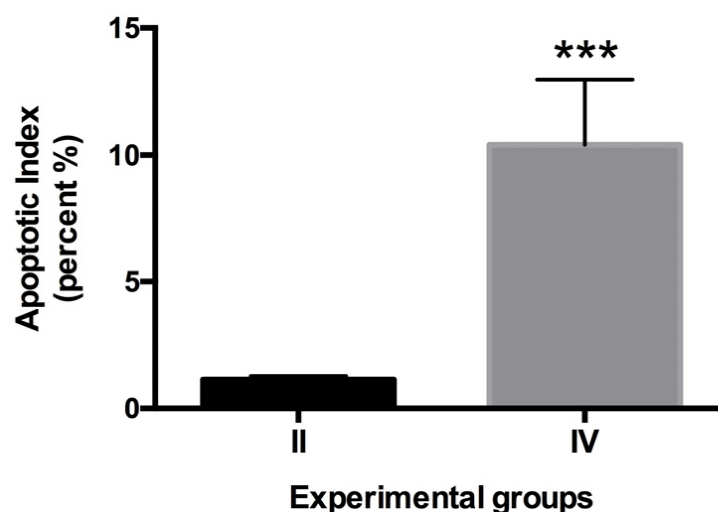


Figure 9. Apoptotic index. The index was higher in group IV (urethane-V) compared with group II (urethane). N = 10, values are expressed as mean percentage of TUNEL positive nuclei \pm SEM (two-tailed Student's *t*-test with Welch's correction $p \leq 0.05$). *** Statistically significant differences between group II versus group IV.

3. Discussion

In the present study, we report that V aerosol delivery interfered with the development of lung adenomas induced by urethane. The decrease in the area and the number of tumors was the result of increasing apoptosis of the tumor cells evaluated by TUNEL; however, no effect was observed in the PCNA proliferation marker. No respiratory clinical compromise was observed in the mice exposed to aerosolized V, and only a difference in weight gain was notorious in the V-exposed groups.

Vanadium as an antineoplastic agent has been previously explored. Köpf-Maier et al. found that vanadocene dichloride (VDC) reduces cell proliferation in leukemia tumor cells [23]. In female Sprague Dawley rats, Thompson et al., in MNU-1 (1-methyl-1-nitrosurea)-induced mammary carcinogenesis, show that supplementation with vanadium sulfate reduced the incidence and the average amount of neoplasms [24]. Other studies from Köpf-Maier's group report that the antitumor activity of VDC on the Fluid Erlich ascites tumor is because of its heterochromatin accumulation [25], mitotic aberration induction, transitory mitosis suppression, and reversible cell accumulation in the late S and G2 phases [23]. Bishayee et al. [26] suggest that the antineoplastic action of VDC might be the result of the effect on the antioxidant status in the liver and the modulation of drug metabolism enzymes of phases I and II. Sankar-Ray et al. suggested the suppression of cell proliferation, induction of apoptosis, and DNA cross-links reduction as other possible antineoplastic mechanisms. In our experimental model, an increase in apoptotic cells was observed, but not in PCNA proliferation biomarkers [27].

These results suggest that apoptosis could be the mechanisms by which V is acting on the adenomas. Recently, Rozzo et al. [15] reported the effect of V compounds in the melanoma A375 cell line in which apoptosis is observed, as well as the arrest of cell cycle in two different phases, probably by different mechanisms. The findings reported here suggest that V in aerosol delivery could be acting by inducing apoptosis and possible the tumors' cell cycle arrest [28–30].

Lu et al. demonstrated that some synthetic V complexes showed pro-apoptotic activities in MGC803 (human gastric cancer cell line) cells related to the increase in proteins such as Bax, caspases 3 and 9, as well as the decrease in Bcl2 [31]. On the other hand, Xi et al. reported the induction of apoptotic cell death in A549 and BEAS-2B lung cancer lines associated with the overexpression of caspase 3 induced by the exposure to V nanoparticles [32].

The generation of reactive oxygen species (ROS) [28] and their effect on the neoplastic cells such as: DNA damage, oxidative alterations of other cellular organelles leading to apoptosis, and different types of cell death mechanisms, could explain the antineoplastic effects of V compounds [5].

Aerosol Delivery

In a variety of respiratory diseases, the aerosol delivery of drug treatments has been used with good results [33]. The best examples are inhaled steroids for asthma, which reduce the symptoms and the systemic effects of steroids [21]. Hamzamy et al. reported the intratracheal administration of temozolomide in gold nanoparticles or liposomes as antineoplastic carriers for the treatment of urethane-induced lung adenomas in mice [18]. Gagnadoux et al., with gemcitabine delivered by the same route, reported the potential use of aerosol delivery for lung cancer treatment [20]. The aerosol delivery of chemotherapy for lung cancer treatment in patients with non-small cell lung carcinoma (NSCLC) was reported. 5-fluorouracil (5-FU) was delivered by an ultrasonic nebulizer in two different situations: one in patients prior to surgical resection, in which the authors demonstrated that the concentration of the 5-FU was 5 to 15 times higher in the tumor than in the normal lung tissue, and two, conducted in patients with unresectable tumor in which the 5-FU was also administered by aerosol delivery, two to three times a week, reporting less pulmonary or systemic side effects. Additionally, the main agent used in the therapeutic schemes for lung cancer, cisplatin, was delivered by inhalation with less systemic side effects and with promising preclinical results [34]. With the urethane model, Abdelaziz et al. reported the reduction in lung tumors in BALB/c mice by the inhalation of lactoferrin/Chondroitin-Functionalized Monoolein Nanocomposites, supporting the use of inhalation as a possible route for lung cancer treatment, stressing that by inhalation route the agent employed in the treatment reaches higher concentrations in the tumors [35].

In our study, with whole body exposure, the regression of the adenomas was almost complete, observing some areas of peribronchiolar inflammation with no clinical effects observed in the mice, only a weight increase in V-exposed groups, which could be explained by the anabolic activity reported for V [36].

Vanadium has been reported as a possible chemotherapeutic agent for different types of neoplasms. Some antineoplastic drugs have been administered by aerosol delivery with promising results [20,32]. Here, we propose V as a potential antineoplastic agent for lung cancer by aerosol delivery that will reduce the number of tumor cells and possibly the systemic side effects reported for V. Other V compounds need further analysis to find the dose and the best protocol for the administration for this element, which opens another possible treatment for NSCLC.

4. Materials and Methods

4.1. Animals

Forty CD-1 adult male mice weighing 33–35 g were housed in hanging plastic cages (10 animals per cage), kept in an animal facility (with an average temperature of 21 °C, 57% humidity and controlled lighting –12:12 h light/dark regime), and fed with Rodent Laboratory chow (PMI nutrition international, Brentwood, MO, USA and Agribrands Purina, Cuautitlan, Mexico) and filtered water ad libitum. Mice were obtained from the vivarium at the School of Medicine, UNAM, and managed according to the Mexican official norm NOM-062-ZOO-1999 for the production, care, and use of laboratory animals. The project was reviewed and approved by the Research and Ethical Committee from the School of Medicine (#04-2005).

4.2. Experimental Protocol

Adult male mice were randomly assigned into four groups of 10 mice each: group I (negative control) inhaled saline 0.9% during the exposures; group II (urethane alone as positive control), received a single dose (ip) of urethane 1mg/g (ethyl carbamate, 99% purity,

Sigma Aldrich, St. Louis, MO, USA) in accordance with previous studies using the urethane-induced lung tumorigenesis model [37]; group III (vanadium) inhaled V_2O_5 (0.02 mol/L) (99.99%, Sigma, St. Louis, MO, USA) in saline 1h twice a week (Tuesday and Thursday) for the 8 weeks of exposure time; and group IV (urethane and V) was as in groups II (urethane alone) and III (vanadium). At the end of the 8-week exposure, mice were anesthetized with (ip) lethal dose of pentobarbital sodium (PiSa Pharmaceutical, Guadalajara, Jalisco, México) 0.3 mg/mL and perfused via aorta with saline followed by 4% paraformaldehyde, whereas the lungs were fixed intratracheally with 4% paraformaldehyde at Total Lung Capacity (TLC) [38].

4.3. Vanadium Exposure and Cardiothoracic Block Dissection

Mice of the V-exposed groups (III and IV) inhaled 1h twice a week in an acrylic box chamber measuring 45 cm × 21 cm × 35 cm (3.3 L total volume), that could house 20 mice per session. An ultra-nebulizer DeVillbiss Ultraneb 99 (DeVillbiss Healthcare, Somerset, PA, USA) system was used to nebulize the vanadium solution at a flow rate of 10 L/min; according to the manufacturer's provided information, about 80% of the aerosolized particles reaching the mice would be expected to have a mass median aerodynamic diameter (MMAD) of 0.5–5 μ m. The concentration of vanadium in the chamber was quantified as follows: a filter was placed at the external outlet of the nebulizer during the entire exposure period and samples were collected at a flow rate of 10 L/min. The filter was removed and weighed after each exposure; the V on each filter was quantified as follows: six-filters per inhalation exposures were evaluated. The source of the fog was located at the top of the chamber to ensure a homogeneous exposure. Mice behavior was always observed to detect any changes. As it has been reported in earlier studies, the final concentration in the chamber was 1.56 mg V/m³ [36] and it is in the range of the World Health Organization (0.01–60 mg/m³) for V concentrations detected in occupational exposures [39]. The V concentration in the blood was analyzed by mass spectrometry of induction-coupled plasma (ICP-MS) using a Bruker equipment, model Aurora M90, with coupled autosampler (Bruker Corp., Billerica, MA, USA). The concentration of the metal was 436 ppb or nanograms of V per of dry weight tissue (ng/g).

4.4. Tissue Sampling and Preparation

Experimental and control groups were sacrificed at the end of the exposures (8 Wk). Animals were anesthetized with sodium pentobarbital aqueous solution of (PiSa Pharmaceutical, Guadalajara, Jalisco, México) 0.3 mg/mL (ip) and perfused via aorta with saline, followed by 4% paraformaldehyde (pH 7.4) in phosphate buffer. The cardiopulmonary block was removed, and then the lungs were dissected and processed for paraffin wax embedding; 5 μ m thickness tissue sections were obtained and stained with hematoxylin-eosin, and proved for immunohistochemical evaluation with anti-PCNA antibody and TUNEL assay. Changes were assessed with a light microscope BX51 (Olympus, Miami, FL, USA). Samples were photographed with a digital camera attached to the microscope (Media Cybernetics Inc., Bethesda, MD, USA). The number and area of the tumors were measured with Motic Images 2.0 software (Motic, Kowloon Bay, Kowloon, Hong Kong).

4.5. Immunohistochemistry for PCNA

Tissue sections were placed in poly-L-lysine (SIGMA, St Louis, MO, USA) coated slides. Antigen retrieval was achieved by incubation in a citrate buffer (pH 7.4) at 103425 Pa for 3 min, after which the slides were washed in phosphate-buffered saline (PBS). Endogenous peroxidase was blocked with 3% H₂O₂ (J.T. Baker, Phillipsburg, NJ, USA) for 10 min. The sections were rinsed several times with PBS-Albumin, washed for 10 min in PBS, (MP Biomedicals Inc, Kuwait city, Kuwait) and incubated for 1 h at 37 °C in rabbit monoclonal anti-PCNA (Abcam, Cambridge, MA, USA), and diluted 1:100 in PBST- (PBS with 0.1% Tween 20 and Albumin). The sections were washed in PBS and incubated for 30 min at 37 °C with the biotinylated universal link secondary antibody (Dako, Carpinteria, CA,

USA), rinsed several times in PBS, and incubated for 30 min at 37 °C in HRP streptavidin complex (Dako, Carpinteria, CA, USA). Immunoreactivity was visualized by incubation in 0.05% 3,3'-diaminobenzidine tetrahydrochloride (Zymed Laboratories Inc, San Francisco, CA, USA). Samples skipping primary antibody were also included as negative controls. Immunoreactivity to PCNA-exposed lungs was measured in tissue sections to calculate the proliferation index in the adenomas; the total adenomas were evaluated from the slides of the lung of each animal and the number of positive nuclei were also counted; positive nuclei were considered when an ochre color stain was observed when the developer for the reaction was diaminobenzidine. The evaluation was completed with an image analyzer, using the software Image-Pro-Plus version 6.0. (Media Cybernetics Inc., Silver Spring, MD, USA) coupled to a digital camera (Evolution MP Color, Media Cybernetics Inc., Silver Spring, MD, USA) on a light microscope Olympus BX51 (Olympus America Inc., Melville, NY, USA).

Proliferative index (PI) was determined by a relation between the number of positive nuclei per adenoma by the total number of cells in each tumor by 100.

4.6. TUNEL Assay

The enzymatic TUNEL assay (TdT-mediated dUPT-biotin nick end labeling) (Dead-End™ Colorimetric TUNEL System, Promega Corp., Madison, WI, USA) was used to evaluate the apoptotic index. The assay identifies DNA strand breaks by marking the free 3'-OH terminal, with biotinylated desoxyuridine with the enzymatic reaction with terminal deoxynucleotidyl transferase (tdT). The biotin signaling is detected by the streptavidin-marked nuclei with the HRP enzyme bound by the biotinylated nucleotides which are visualized with HRP,3,3'-diaminobenzidine (DAB). The apoptotic nuclei are observed in ochre color in the light microscope. The assay was performed according to the providers' indications. The slides were counterstained with light green to increase the visibility of the apoptotic nucleus.

The apoptotic index (AI) was calculated in 40X photomicrographs from the different groups. Five fields randomly were selected. TUNEL positive nuclei were counted within the tumors and the total nuclei from each tumor. The index was calculated with the formula: Total amount of marked nuclei/ total nuclei X 100. The total nuclei were counted in Feulgen-stained slides [40]. Apoptotic index was compared between Group II and Group IV.

4.7. Statistical Analysis

In the different experimental groups comparison of the number of the tumors was carried out with an analysis of variance (ANOVA) with Tukey's post hoc test, whereas the analysis of the tumors area, the PI and AI was carried out with Student's *t*-test with Welch's correction (GraphPad Prism Software V 6.0, La Jolla, CA, USA). Differences were considered when $p < 0.05$.

5. Conclusions

Inhaled vanadium decreases the number and size of urethane-induced lung adenomas in mice by inducing apoptosis of the tumor cells, and with no observed clinical effects.

A limitation of this study was that the effect of V was only analyzed at a single point. It would be interesting to evaluate the effects of V overtime, to establish a wider picture of its beneficial and side effects.

Further studies about the mechanisms that lead to apoptotic cell death overtime in this model would be of interest, as well as if other types of cell death could be involved in this process.

In addition, to study if V interferes with urethane's metabolism throughout the whole experiment, we would add more information about the effects observed in this study.

Author Contributions: Conceptualization, N.L.-V.; methodology, N.L.-V. and M.R.-L.; formal analysis, N.L.-V.; investigation, N.L.-V. and M.R.-L.; resources, N.L.-V. and T.I.F.; writing—original draft preparation, N.L.-V.; writing—review and editing, N.L.-V. and T.I.F.; project administration, T.I.F. All authors have read and agreed to the published version of the manuscript.

Funding: This research received no external funding.

Acknowledgments: The authors thank Raquel Guerrero-Alquicira for the tissue processing and to Armando Zepeda-Rodríguez and Francisco Pasos-Nájera for the artwork with the figures, all from the Departamento de Biología Celular y Tisular, Facultad de Medicina, UNAM. Alejandra Núñez-Fortoul edited English of the final version of the manuscript.

Conflicts of Interest: The authors declare no conflict of interest.

References

1. Siegel, R.L.; Miller, K.D.; Jemal, A. Cancer Statistics, 2017. *CA Cancer J. Clin.* **2017**, *67*, 7–30. [[CrossRef](#)]
2. McCarthy, W.J.; Meza, R.; Jeon, J.; Moolgavkar, S.H. Chapter 6: Lung cancer in never smokers: Epidemiology and risk prediction models. *Risk Anal.* **2012**, *32* (Suppl. 1), S69–S84. [[CrossRef](#)]
3. Green, L.S.; Fortoul, T.I.; Ponciano, G.; Robles, C.; Rivero, O. Bronchogenic cancer in patients under 40 years old. The experience of a Latin American country. *Chest* **1993**, *104*, 1477–1481. [[CrossRef](#)]
4. Jamal-Hanjani, M.; Wilson, G.A.; McGranahan, N.; Birkbak, N.J.; Watkins, T.B.K.; Veeriah, S.; Shafi, S.; Johnson, D.H.; Mitter, R.; Rosenthal, R.; et al. Tracking the Evolution of Non-Small-Cell Lung Cancer. *N. Engl. J. Med.* **2017**, *376*, 2109–2121. [[CrossRef](#)] [[PubMed](#)]
5. Guerrero-Palomo, G.; Rendon-Huerta, E.P.; Montano, L.F.; Fortoul, T.I. Vanadium compounds and cellular death mechanisms in the A549 cell line: The relevance of the compound valence. *J. Appl. Toxicol.* **2019**, *39*, 540–552. [[CrossRef](#)] [[PubMed](#)]
6. Blumenthal, G.M.; Karuri, S.W.; Zhang, H.; Zhang, L.; Khozin, S.; Kazandjian, D.; Tang, S.; Sridhara, R.; Keegan, P.; Pazdur, R. Overall response rate, progression-free survival, and overall survival with targeted and standard therapies in advanced non-small-cell lung cancer: US Food and Drug Administration trial-level and patient-level analyses. *J. Clin. Oncol.* **2015**, *33*, 1008–1014. [[CrossRef](#)] [[PubMed](#)]
7. Jamal-Hanjani, M.; Quezada, S.A.; Larkin, J.; Swanton, C. Translational implications of tumor heterogeneity. *Clin. Cancer Res.* **2015**, *21*, 1258–1266. [[CrossRef](#)] [[PubMed](#)]
8. Suda, K.; Rozeboom, L.; Rivard, C.J.; Yu, H.; Ellison, K.; Melnick, M.A.C.; Hinz, T.K.; Chan, D.; Heasley, L.E.; Politi, K.; et al. Therapy-induced E-cadherin downregulation alters expression of programmed death ligand-1 in lung cancer cells. *Lung Cancer* **2017**, *109*, 1–8. [[CrossRef](#)]
9. Kemp, C.J. Animal Models of Chemical Carcinogenesis: Driving Breakthroughs in Cancer Research for 100 Years. *Cold Spring Harb. Protoc.* **2015**, *2015*, 865–874. [[CrossRef](#)]
10. Gurley, K.E.; Moser, R.D.; Kemp, C.J. Induction of Lung Tumors in Mice with Urethane. *Cold Spring Harb. Protoc.* **2015**, *2015*, pdb-prot077446. [[CrossRef](#)] [[PubMed](#)]
11. Parra, E.R.; Alveno, R.A.; Faustino, C.B.; Correa, P.Y.; Vargas, C.M.; de Moraes, J.; Rangel, M.P.; Velosa, A.P.; Fabro, A.T.; Teodoro, W.R.; et al. Intranasal Administration of Type V Collagen Reduces Lung Carcinogenesis through Increasing Endothelial and Epithelial Apoptosis in a Urethane-Induced Lung Tumor Model. *Arch. Immunol. Ther. Exp. (Warsz)* **2016**, *64*, 321–329. [[CrossRef](#)] [[PubMed](#)]
12. Levine, A.J. The Evolution of Tumor Formation in Humans and Mice with Inherited Mutations in the p53 Gene. *Curr. Top. Microbiol. Immunol.* **2017**, *407*, 205–221. [[CrossRef](#)] [[PubMed](#)]
13. Petanidis, S.; Kioseoglou, E.; Hadzopoulou-Cladaras, M.; Salifoglou, A. Novel ternary vanadium-betaine-peroxido species suppresses H-ras and matrix metalloproteinase-2 expression by increasing reactive oxygen species-mediated apoptosis in cancer cells. *Cancer Lett.* **2013**, *335*, 387–396. [[CrossRef](#)] [[PubMed](#)]
14. Rehder, D. The role of vanadium in biology. *Metallomics* **2015**, *7*, 730–742. [[CrossRef](#)] [[PubMed](#)]
15. Rozzo, C.; Sanna, D.; Garribba, E.; Serra, M.; Cantara, A.; Palmieri, G.; Pisano, M. Antitumoral effect of vanadium compounds in malignant melanoma cell lines. *J. Inorg. Biochem.* **2017**, *174*, 14–24. [[CrossRef](#)]
16. Kowalski, S.; Hac, S.; Wyrzykowski, D.; Zauszkiewicz-Pawlak, A.; Inkielewicz-Stepniak, I. Selective cytotoxicity of vanadium complexes on human pancreatic ductal adenocarcinoma cell line by inducing necroptosis, apoptosis and mitotic catastrophe process. *Oncotarget* **2017**, *8*, 60324–60341. [[CrossRef](#)]
17. Paredes Aller, S.; Quittner, A.L.; Salathe, M.A.; Schmid, A. Assessing effects of inhaled antibiotics in adults with non-cystic fibrosis bronchiectasis—Experiences from recent clinical trials. *Expert Rev. Respir. Med.* **2018**, *12*, 769–782. [[CrossRef](#)]
18. Hamzawy, M.A.; Abo-Youssef, A.M.; Salem, H.F.; Mohammed, S.A. Antitumor activity of intratracheal inhalation of temozolomide (TMZ) loaded into gold nanoparticles and/or liposomes against urethane-induced lung cancer in BALB/c mice. *Drug Deliv.* **2017**, *24*, 599–607. [[CrossRef](#)]
19. Carafa, M.; Marianecchi, C.; Donatella, P.; D’i Marzio, L.; Celia, M.; Fresta, F.; Alhaique, F. Novel concept in pulmonary delivery. In *Chronic Obstructive Pulmonary Disease-Current Concept and Practice*; Ong, K.C., Ed.; IntechOpen Limited: London, UK, 2012.

20. Gagnadoux, F.; Pape, A.L.; Lemarie, E.; Lerondel, S.; Valo, I.; Leblond, V.; Racineux, J.L.; Urban, T. Aerosol delivery of chemotherapy in an orthotopic model of lung cancer. *Eur. Respir. J.* **2005**, *26*, 657–661. [CrossRef]
21. Barnes, P.J. Inhaled Corticosteroids. *Pharmaceuticals* **2010**, *3*, 514–540. [CrossRef]
22. Borghardt, J.M.; Kloft, C.; Sharma, A. Inhaled Therapy in Respiratory Disease: The Complex Interplay of Pulmonary Kinetic Processes. *Can. Respir. J.* **2018**, *2018*, 2732017. [CrossRef] [PubMed]
23. Kopf-Maier, P.; Wagner, W.; Hesse, B.; Kopf, H. Tumor inhibition by metallocenes: Activity against leukemias and detection of the systemic effect. *Eur. J. Cancer* **1981**, *17*, 665–669. [CrossRef]
24. Thompson, H.J.; Chasteen, N.D.; Meeker, L.D. Dietary vanadyl(IV) sulfate inhibits chemically-induced mammary carcinogenesis. *Carcinogenesis* **1984**, *5*, 849–851. [CrossRef] [PubMed]
25. Kopf-Maier, P.; Wagner, W.; Liss, E. Induction of cell arrest at G1/S and in G2 after treatment of Ehrlich ascites tumor cells with metallocene dichlorides and cis-platinum in vitro. *J. Cancer Res. Clin. Oncol.* **1983**, *106*, 44–52. [CrossRef] [PubMed]
26. Bishayee, A.; Oinam, S.; Basu, M.; Chatterjee, M. Vanadium chemoprevention of 7,12-dimethylbenz(a)anthracene-induced rat mammary carcinogenesis: Probable involvement of representative hepatic phase I and II xenobiotic metabolizing enzymes. *Breast Cancer Res. Treat* **2000**, *63*, 133–145. [CrossRef]
27. Sankar Ray, R.; Roy, S.; Ghosh, S.; Kumar, M.; Chatterjee, M. Suppression of cell proliferation, DNA protein cross-links, and induction of apoptosis by vanadium in chemical rat mammary carcinogenesis. *Biochim. Biophys. Acta* **2004**, *1675*, 165–173. [CrossRef] [PubMed]
28. Evangelou, A.M. Vanadium in cancer treatment. *Crit. Rev. Oncol. Hematol.* **2002**, *42*, 249–265. [CrossRef]
29. Mateos-Nava, R.A.; Rodriguez-Mercado, J.J.; Altamirano-Lozano, M.A. Premature chromatid separation and altered proliferation of human leukocytes treated with vanadium (III) oxide. *Drug Chem. Toxicol.* **2017**, *40*, 457–462. [CrossRef] [PubMed]
30. Leon, I.E.; Porro, V.; Di Virgilio, A.L.; Naso, L.G.; Williams, P.A.; Bollati-Fogolin, M.; Etcheverry, S.B. Antiproliferative and apoptosis-inducing activity of an oxidovanadium(IV) complex with the flavonoid silibinin against osteosarcoma cells. *J. Biol. Inorg. Chem.* **2014**, *19*, 59–74. [CrossRef]
31. Lu, L.P.; Suo, F.Z.; Feng, Y.L.; Song, L.-L.; Li, Y.; Li, Y.-J.; Wang, K.-T. Synthesis and biological evaluation of vanadium complexes as novel anti-tumor agents. *Eur. J. Med. Chem.* **2019**, *176*, 1–10. [CrossRef]
32. Xi, W.S.; Tang, H.; Liu, Y.Y.; Liu, C.Y.; Gao, Y.; Cao, A.; Liu, Y.F.; Chen, Z. Cytotoxicity of vanadium oxide nanoparticles and titanium dioxide-coated vanadium oxide nanoparticles to human lung cells. *J. Appl. Toxicol.* **2020**, *40*, 567–577. [CrossRef] [PubMed]
33. Chen, Y.; Zhao, Y.; Dai, C.L.; Liang, Z.; Run, X.; Iqbal, K.; Liu, F.; Gong, C.X. Intranasal insulin restores insulin signaling, increases synaptic proteins, and reduces Abeta level and microglia activation in the brains of 3xTg-AD mice. *Exp. Neurol.* **2014**, *261*, 610–619. [CrossRef]
34. Gagnadoux, F.; Hureauux, J.; Vecellio, L.; Urban, T.; Le Pape, A.; Valo, I.; Montharu, J.; Leblond, V.; Boisdron-Celle, M.; Lerondel, S.; et al. Aerosolized chemotherapy. *J. Aerosol. Med. Pulm. Drug Deliv.* **2008**, *21*, 61–70. [CrossRef]
35. Abdelaziz, H.M.; Elzoghby, A.O.; Helmy, M.W.; Abdelfattah, E.A.; Fang, J.Y.; Samaha, M.W.; Freag, M.S. Inhalable Lactoferrin/Chondroitin-Functionalized Monoolein Nanocomposites for Localized Lung Cancer Targeting. *ACS Biomater. Sci. Eng.* **2020**, *6*, 1030–1042. [CrossRef] [PubMed]
36. Fortoul, T.I.; Rojas-Lemus, M.; Rodriguez-Lara, V.; Gonzalez-Villalva, A.; Ustarroz-Cano, M.; Cano-Gutierrez, G.; Gonzalez-Rendon, S.E.; Montano, L.F.; Altamirano-Lozano, M. Overview of environmental and occupational vanadium exposure and associated health outcomes: An article based on a presentation at the 8th International Symposium on Vanadium Chemistry, Biological Chemistry, and Toxicology, Washington DC, August 15–18, 2012. *J. Immunotoxicol.* **2014**, *11*, 13–18. [CrossRef] [PubMed]
37. Roomi, M.W.; Roomi, N.W.; Kalinovsky, T.; Rath, M.; Niedzwiecki, A. Chemopreventive Effect of a Novel Nutrient Mixture on Lung Tumorigenesis Induced by Urethane in Male A/J Mice. *Tumori. J.* **2009**, *95*, 508–513. [CrossRef]
38. Fortoul, T.I.; Soto-Mota, A.; Rojas-Lemus, M.; Rodriguez-Lara, V.; Gonzalez-Villalva, A.; Montano, L.F.; Paez, A.; Colin-Barenque, L.; Lopez-Valdez, N.; Cano-Gutierrez, G.; et al. Myocardial connexin-43 and N-Cadherin decrease during vanadium inhalation. *Histol. Histopathol.* **2016**, *31*, 433–439. [CrossRef] [PubMed]
39. Costigan, M.C.; Dobson, R. *Vanadium Pentoxide and Other Inorganic Vanadium Compounds*; World Health Organization & International Programme on Chemical Safety 2001; World Health Organization: Geneva, Switzerland, 2001. Available online: <https://apps.who.int/iris/handle/10665/42365> (accessed on 20 August 2021).
40. Chieco, P.; Derenzini, M. The Feulgen reaction 75 years on. *Histochem. Cell Biol.* **1999**, *111*, 345–358. [CrossRef]